Radiation-induced electrical degradation in crystalline Al_2O_3

Xiang-Fu Zong, Cheng-Fu Shen, Song Liu, Zhong-chi Wu, and Yi Chen
Department of Materials Science and Engineering, Fudan University, Shanghai 200433, China

Y. Chen*
Oak Ridge National Laboratory, Solid State Division, P.O. Box 2008, Oak Ridge, Tennessee 37831-6031

B. D. Evans
Boeing Defense and Space Group, P.O. Box 3999, MS 9E-XW, Seattle, Washington 98124-2499

R. Gonzalez
Universidad Carlos III, Departamento de Ingenieria, Escuela Politecnica Superior, Avda. del Mediterraneo, 20, 28913 Leganes, Madrid, Spain

C. H. Sellers
Idaho National Engineering Laboratory, P.O. Box 1625, Idaho Falls, Idaho 83415-2211
(Received 20 October 1993; revised manuscript received 19 January 1994)

Recent studies, simulating the behavior of insulating materials in a fusion device environment, show that under concurrent applications of radiation, applied electric field, and elevated temperature, they suffer degradation of their electrical properties. The goal of the present study is to address the mechanism of this radiation-induced electrical degradation and the defects involved. Our results show that when an Al_2O_3 crystal under a moderate electric field is irradiated with 1.8 MeV electrons at 773 K, the dc conductivity during and after irradiation increases rapidly above a critical dose and saturates after the conductivity increases by a factor of 10^3. There are two main conclusions. First, the electrical degradation is due to the charge of the electrons and holes created during radiation, rather than due to displacements of indigenous ions by elastic collisions with the energetic electrons. Second, the defects attending the observed electrical degradation are dislocations. Transmission electron microscopy studies revealed regions of large dislocation density distributed nonuniformly throughout the degraded area, with an *overall* average density of $\sim 10^9$ cm^{-2}, as opposed to $\sim 10^4$ cm^{-2} in regions which were not electron irradiated nor subjected to an electric field. The concentration of point defects, as characterized by optical absorption and electron paramagnetic resonance, was below detectable limit. In addition, no second phase was observed.

I. INTRODUCTION

It has recently been reported that experimental simulations of hostile environments surrounding several key components in fusion power systems produced adverse effects on the electrical properties of insulating ceramics.[1-4] The *simultaneous* applications of *Rad*iation with energetic particles, *E*lectric field, and elevated *T*emperature (to be abbreviated hereafter as Rad-E-T) to α-Al_2O_3 for an extended period of time led to electrical degradation of the material. (It is emphasized that all three applications are concurrent.) The general features are illustrated in Fig. 1. Under a moderate electric field at an elevated temperature, α-Al_2O_3 does not experience a change in electrical conductivity or electrical degradation, as shown by the flat dotted line. However, when subjected to irradiations with energetic particles, such as electrons or neutrons, it experiences an increase in the electrical conductivity. This incremental increase, due to *R*adiation *I*nduced *C*onductivity (RIC), is proportional to the dose rate and independent of the accumulated dose (for the classic paper on this subject, see Ref. 5). Under constant conditions of Rad-E-T, RIC remains unchanged for a long period, as shown in the figure. In recent Rad-E-T experiments carried out to higher doses,[1] it was reported that beyond some critical dose the electrical con-

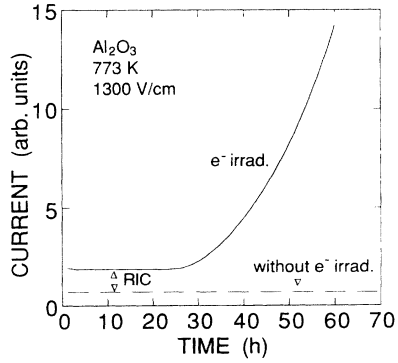

FIG. 1. Main features of electrical current vs time during electron irradiation of Al_2O_3 at an elevated temperature with an applied electric field. The current increases at a critical dose. This critical dose corresponds to ~30 h of Van de Graaff irradiation in Ref. 1. The dotted line corresponds to the current level with no irradiations.

ductivity began to increase, signaling the onset of what was reported to be an electrical breakdown. This increase in conductivity, over and above RIC, continued without limit with irradiation dose until the material could no longer be regarded as an electrical insulator. The removal of radiation did not return the conductivity to its preirradiation level, in contrast to RIC. Furthermore, the degraded ceramic insulator could not be readily annealed or otherwise returned to its original low conductivity. The increase in conductivity was reported to be attended by a visible coloration.[3] The experimental results were interpreted as showing that the electrical breakdown was related to exposure to energetic electrons during Rad-E-T. This behavior poses a serious challenge for fusion power systems, which require electrical insulating integrity for various applications, including diagnostic ports, radio frequency and neutral beam injectors, magnetic coil insulators, and toroidal current breaks.

This unexpected phenomenon emphasizes the importance of *in situ* studies, as opposed to post-mortem investigations. In view of the importance of this phenomenon pertaining to advanced energy devices, we have conducted a study in order to obtain a fundamental understanding of the mechanism of the electrical degradation and the defects involved. For reasons which will become more obvious later, this phenomenon will be referred to in a more general term—radiation-induced electrical degradation (RIED), rather than radiation-enhanced electrical breakdown, as has been referred to in the past.[1,3]

II. EXPERIMENTAL PROCEDURES

High-purity single crystals of α-Al_2O_3 were obtained from both the Shanghai Institute of Optics and Fine Mechanics (SIOFM) and the Union Carbide Corporation (UCC). Impurity elements such as Si, K, Mg, Fe, Ca in the SIOFM crystals were reported to us to have impurity concentrations up to 50 ppm. The SIOFM crystal was grown by the temperature gradient technology method. MgO single crystals were grown at the Oak Ridge National Laboratory (ORNL) by the arc fusion method.

One sample was obtained from SIOFM, with the c axis perpendicular to the broad surface and parallel to the applied electric field E in RIED studies. The thickness was 0.85 mm and the diameter was 17 mm. Platinum contacts were deposited on the sample by sputtering from a Pt foil in vacuum. For intimate contact with the Pt, the sample was held at ~475 K during the deposition. The thickness of the sputtered Pt is estimated to be 100–200 nm. Additional electrical contacts were an Au ring and disk; two large masses of copper were used for thermal contact (see Fig. 2). The top copper ring also served to collimate the electron beam, so that the periphery of the sample was shielded from the electron beam. The diameter of the collimated beam was 9.5 mm. An auxiliary heater ring and a dc voltage source supplied the necessary temperature and voltage requirements. Another sample, purchased from the Union Carbide Corporation, had the same crystal orientation and a thickness of 1.0 mm. It came optically polished and was used for high-dose electron irradiation at room temperature without an

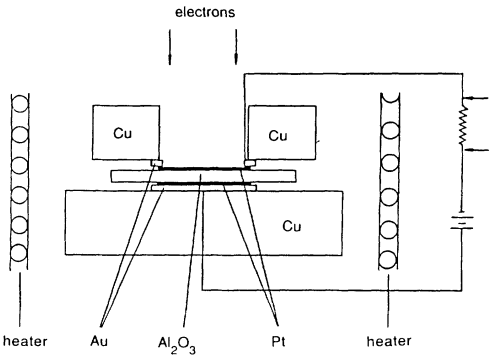

FIG. 2. Diagram of the experimental setup.

applied electric field. Four UCC sapphire crystals (two with surfaces parallel to the c axis, and two with surfaces perpendicular to the c axis), and two MgO crystals were neutron irradiated at two different temperatures.

The electron irradiaion was carried out using a vertical Van de Graaff operating at 1.8 MeV at ~$4\mu A/cm^2$. The neutron irradiations were performed at 320 and 480 K in the Low-Temperature Neutron Irradiation Facility at the Oak Ridge National Laboratory. A Philips EM 430 electron microscope with an operating voltage of 300 KV was used for post-irradiation transmission electron microscope observations. Two samples, with diameter of about 3 mm, were cut from the center and the edge (sheltered by the copper cylinder) of the irradiated disc by ultrasonic cutting (Gatan Model 601). They were then polished to 50 μm by dimpler (Model D500) and were thinned by a dual ion mill (Gatan Model 600) until a small hole appeared. The thin sample around the hole was then studied by transmission electron microscopy (TEM). Optical-absorption measurements were taken with a Perkin-Elmer Lambda 9 spectrophotometer. Electron paramagnetic resonance (EPR) measurements were made on a Varian E-line spectrometer operating at X band with 100-kHz field modulation. The addition of a narrow-tailed quartz dewar inserted into the microwave cavity enabled measurements to be performed at 77 K.

There were several experimental differences between the present work and those reported in Refs. 1 and 3: (1) The present work was carried out in air, whereas the previous studies were carried out "in vacuum." (2) In the present work, the dc electric field was applied parallel to the c direction, whereas no crystal orientation was reported in the previous work. (3) The present dose rate was about a factor of ~20 higher. (4) The total dose was also higher, by about a factor of 10. (5) The sources of the crystals were also different—SIOFM as opposed to Roditi-Union Carbide uv grade.

III. RESULTS AND DISCUSSION

A. Dose-dependent dc electrical conductivity

In this section we provide results which illustrate the electrical characteristics as a function of electron dose. Figure 3 illustrates a semilog plot of the dc conductivity

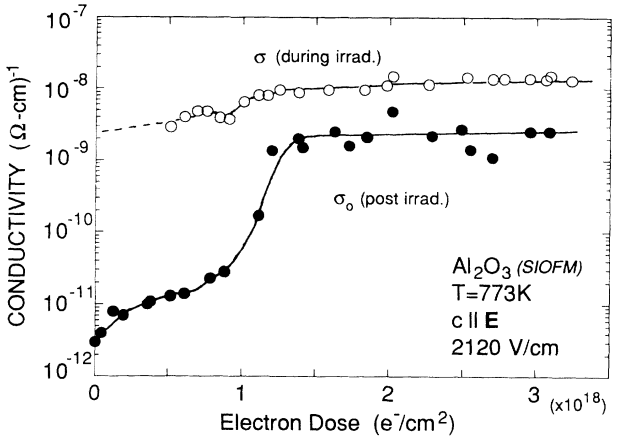

FIG. 3. Semilog plot of conductivity vs electron dose of an Al_2O_3 crystal during irradiation (top curve), and after irradiation followed by stabilization of the current (bottom curve).

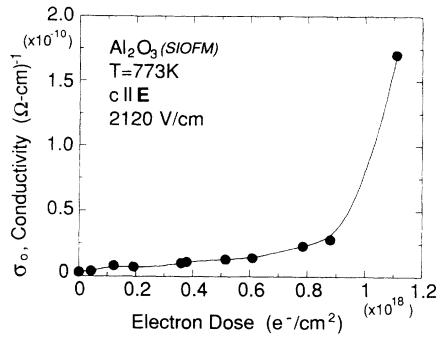

FIG. 4. Linear plot of post-irradiation conductivity vs electron dose of the Al_2O_3 crystal illustrated in Fig. 3 in the early stage of irradiation.

of a SIOFM sapphire crystal at various stages of electron irradiation. The c axis of the crystal was perpendicular to the sample surface, and parallel to the applied electric field and the incoming electron beam. During irradiation the temperature of the sample was held at 773 K and an electric field of 2120 V/cm was maintained. The beam current was about 4 μA/cm^2, or 2.5×10^{13} e cm^{-2} s^{-1}. The top curve illustrates the conductivity during irradiation, represented by σ. Each of the data points in this curve was obtained from the slope of the I-V curve in the first quadrant (to be illustrated by Figs. 5 and 6), and corrected for the zero-voltage current due to the electron beam, as will be described in Sec. III B. These values, which include RIC, depend on the intensity of the beam current, which in the present case was maintained at a constant level. Data were not taken at the beginning; however, the initial conductivity is projected by the dotted line. The beam current was more intense than the previous study, reflected by the nearly flat curve shown in Fig. 3. At this higher dose rate, the conductivity was dominated by RIC.

The post-irradiation conductivity, represented by σ_0 in Fig. 3, reflects values taken after the electron beam had been shut off at various intermediate doses and the conductivity had decayed to a constant value. A waiting period of 4–5 min was adequate to assure a steady-state current. In effect, the σ_0 curve (bottom) reflects the conductivity without RIC. Prior to irradiation, the conductivity σ_0 was about 10^{-12} (ohm cm)$^{-1}$. It then increased slowly with irradiation and hovered around 10^{-11} (ohm cm)$^{-1}$. At a dose of $\sim1.0\times10^{18}$ e/cm^2, the conductivity increases rapidly. (Plotted linearly, this initial portion of the curve is shown in Fig. 4.) The conductivity continued to increase until it reached $\sim10^{-9}$ (ohm cm)$^{-1}$, where it saturated. We extended our total dose to 3.2×10^{18} e/cm^2, but observed no significant conductivity increase beyond 1.2×10^{18} e/cm^2.

The present conductivity results are now compared with those of Ref. 1 and the implications are discussed. Figure 4 resembles the curve of the earlier work. However, it is noted that in the present study the conductivity began to increase at a dose of $\sim1.0\times10^{18}$ e/cm^2, as opposed to $\sim1.0\times10^{17}$ e/cm^2 in the earlier work. This factor of 10 may be significant, but there are differences in the experimental conditions which could account for the discrepancy, including dose rate, ambient conditions (O_2 partial pressure), crystal orientation, and surface conditions. The major differences are dose rate and total dose to which the two studies were carried out: Our total dose was a factor of 11 higher. The implication is significant. Previous experiments[1] were terminated while the conductivity was still increasing and it was assumed that it would increase until the crystal suffered electrical breakdown. Indeed the effect was reported as an electrical breakdown phenomenon. The present study indicates a saturation after an increase of $\sim10^3$ in conductivity. There was no evidence of catastrophic electrical breakdown. Therefore we generalize the effect and call it radiation-induced electrical degradation (RIED).[6]

B. Nonlinear current-voltage characteristics

The current-voltage characteristics after being subjected to Rad-E-T are not always linear. The I-V and I_0-V curves represent those obtained during and after irradiation, respectively. In the former the current I, which is dominated by the RIC and the intense beam current (4 μA/cm^2), is expectedly linear when plotted against V (see Fig. 5). However, there is a zero voltage current. This current is due to the fact that unequal amounts of the beam electrons are in effect deposited on the two opposite sides of the sapphire crystal (see Fig. 2). As mentioned in the previous section, the data given in the top curve of Fig. 3 correspond to values which have been corrected for zero-voltage currents.

In the post-irradiation measurements, the I_0-V curves tend to be linear initially, then become nonlinear after extensive irradiations. At still higher doses, the I_0-V curves again approach linearity. Figure 6 illustrates this effect for three doses. Whereas there was no dramatic increase in the positive direction at 200 V, there was an increase of a factor of 10 in the negative direction for one of the curves. The data given in the lower curve of Fig. 3 correspond to values which are linear (first quadrant in the I_0-V curves).

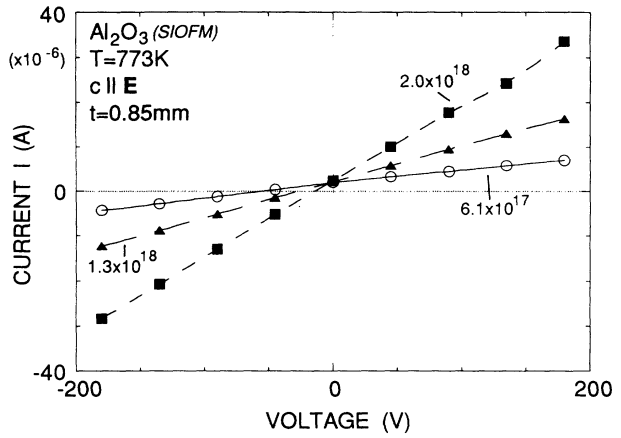

FIG. 5. Current-voltage (I-V) curves during electron irradiation at $\sim 4\mu A/cm^2$ at three different stages of irradiation.

C. Defect characterization: TEM, optical absorption, and magnetic resonance

The one characteristic difference between regions subjected to Rad-E-T and the (shielded) regions not subjected to Rad-E-T was the dislocation density, as characterized by TEM. The dislocation density in the former was enormous, averaging $\sim 10^9$ dislocations/cm^2. However, this distribution was highly nonuniform, such that in some regions the density was orders of magnitude higher than the average. Many low-angle grain boundaries and high density of dislocations were observed in the concentrated regions (see Figs. 7 and 8). On the other hand, the average dislocation density around the peripheral of the sample, which was shielded from direct electron bombardment and not subjected to electric field, was significantly lower: these dislocations were so rare that they were extremely difficult to find, but they did exist. To the best of our estimate, the overall average dislocation density in this shielded region was of the order of, or less than 10^4 cm^{-2}. This magnitude is comparable to what is expected in virgin crystals.

Optical-absorption and electron paramagnetic resonance (EPR) techniques were used to determine the presence of point defects in the crystal after it underwent RIED. There was no visible coloration in the crystal, and no optical-absorption bands associated with well-known lattice vacancies were observed in the range of 700–190 nm. There was increasing scattering as the wavelength decreased, due in part to the rough sample surface after the removal of the Pt contact. However, the sample was too thin to permit additional polishing. Likewise there was no observable room-temperature EPR signal attributable to known point defects, such as the anion vacancy with one electron (the F^+ center).

The lack of coloration also suggests the absence of Mie scattering from particles with dimensions smaller than the wavelength of visible light. Indeed, transmission electron microscopy (TEM) investigations confirmed that there were no observable precipitates. Both the central region of the sample exposed to the electron beam, as

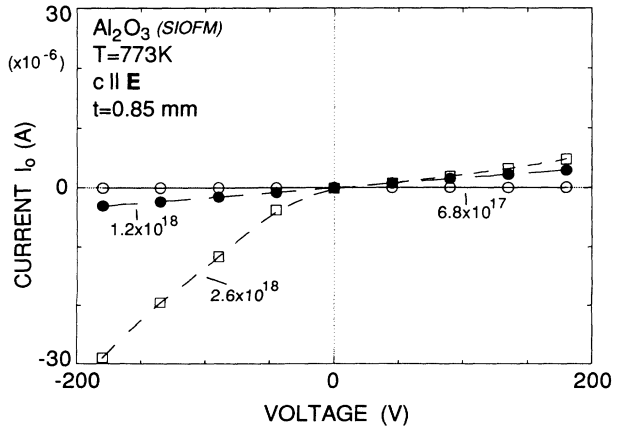

FIG. 6. Post-irradiation current-voltage (I_0-V) curves at three different stages of irradiation.

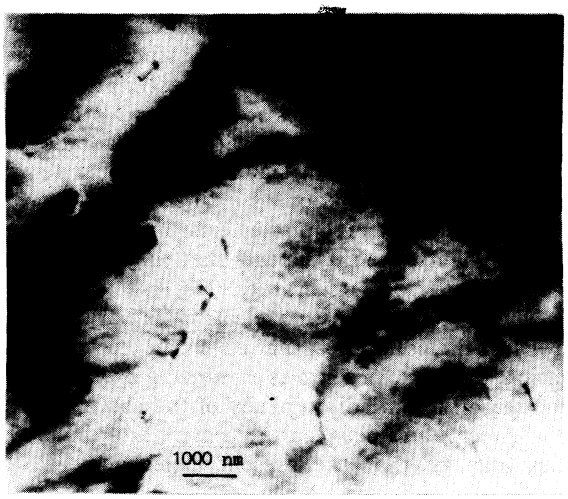

FIG. 7. Transmission electron micrograph showing high density of dislocations in an area previously subjected to Rad-E-T.

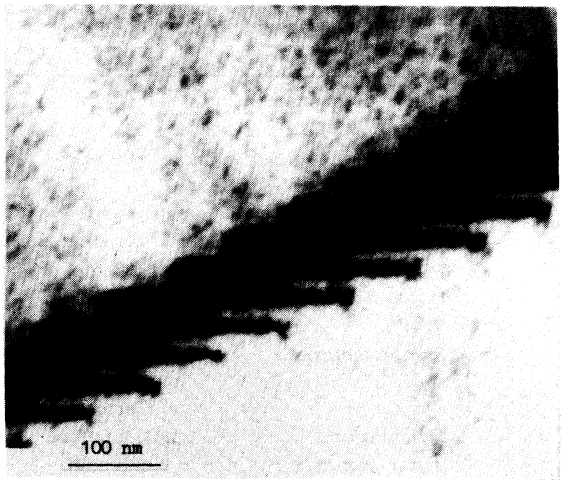

FIG. 8. Transmission electron micrograph of a low-angle boundary of dislocations in an area previously subjected to Rad-E-T.

well as the sheltered region, were imaged by TEM. The absence of precipitates in the present study is in marked contrast with the previous study suggesting the presence of precipitates.[3] Precipitates in MgO and other oxides were known to be formed without irradiation and without an electric field at significantly higher temperatures (>1700 K) in a reducing or inert atmosphere.[7–11] If it is assumed that precipitates exist in the earlier Rad-E-T experiments, then it appears that they are formed at a significantly lower temperature (773 K) but in the presence of an electric field and electron radiation. One is then led to the conclusion that either an electric field, or radiation, or both can serve as a reducing agent.

The reason for the discrepancy of the absence or presence of precipitates between the present and the previous studies may be that the present experiment was performed in air, whereas the earlier work was in vacuum. It is believed that because of the oxygen partial pressure, air serves as an oxidizing agent which effectively counteracts the reducing effect of an electric field, or radiation, or both. Vacuum, on the other hand, behaves more like a reducing environment.

IV. MECHANISMS LEADING TO RIED

In this section various considerations which have implications on the mechanisms leading to RIED are discussed. The understanding of the mechanism of RIED is important, not only from a fundamental point of view, but primarily because it will permit the discrimination of the roles of the various particles in the fusion environment. In this section we present experimental results and phenomenological evidence that the mechanism leading to RIED is due to the roles of electrons and holes created during the irradiation, rather than due to elastic collisions.

The effect of Rad-E-T on the electrical properties of α-Al_2O_3 has been studied using different types of radiations. In order to understand the mechanism of RIED, results from the previous studies are placed in perspective with results from the present studies. Three sets of data are available (see Table I): two are from the electron irradiations already discussed using dc electric fields,[1,3] and the third is from neutron irradiation.[2] The electron irradiations were both carried out using Van de Graaff accelerators, and the neutron irradiations were carried out in a fission reactor, which generates both neutrons and γ rays. All three studies observed substantial enhancement in conductivity at critical doses. We shall assume that all three observations are due to RIED.

In order to compare RIED incurred by electrons and neutrons, the results are converted to the number of particles penetrating per unit area, be it electrons or neutrons. The results are illustrated in Fig. 9. The neutron-irradiation data were reported in terms of days in the reactor at full power, which can be converted to n/cm^2 for neutron energy >0.1 MeV. The earlier electron-irradiation data[1,3] were reported in Gy unit, which can be converted to e/cm^2; for 1.8-MeV electrons, the conversion factor is 2.4×10^{-10} Gy e^{-1} cm^2.[13]

A. Cross-section considerations

A comparison of the cross sections for these irradiations in causing RIED provides a reliable way to determine whether the process is due to atomic displacements by elastic collisions (also known as a knock-on process), or due to roles played by electrons and holes created during irradiation. The goal of the present section is to compare the relative efficiency of electrons versus neutrons in causing RIED, thereby providing a one-to-one comparison between electrons and neutrons. Figure 10 plots the normalized conductivity, σ/σ_0, against e/cm^2, or n/cm^2, for four of the curves shown in Fig. 9. The choice of σ_0

TABLE I. Sample characterization and conditions under which Rad-E-T experiments were performed.

	Hodgson (e^-)	Zong *et al.* (e^-)	Shikama *et al.* (1st) (γ)	Shikama *et al.* (1st) (n^0)	Shikama *et al.* (2nd) (γ)	Shikama *et al.* (2nd) (n^0)
Dose rate ($\times10^{13}$ cm^{-2}s^{-1})	0.12	2.5	1.2	34	2.2	150
Total dose ($\times10^{18}$ cm^{-2})	0.28	3.2	100	2820	91	6300
RIC (Ω cm)$^{-1}$	1.65×10^{-8}	2.9×10^{-9}	6.5×10^{-8}		1.19×10^{-8}	
Electric field (V/cm)	1300 (dc)	2120 (dc)	5 (ac)		5000 (dc)	
T (K)	773	773	600–630		770–800	
Sample source	Single Roditi-Union Carbide	Single SIOFM	Single Kyocera		Polycrystalline Kyocera	
Orientation	not reported	$c\|\|\mathbf{E}$	$c\|\|\mathbf{E}$		Polycrystalline	
Total impurity (ppm)	$\sim10^2$ (?)	20–50	1000		5000	
Sample geometry (mm)	$5\times5\times1$	$17\phi\times0.85$	$8\phi\times1$		$8\phi\times0.5$	

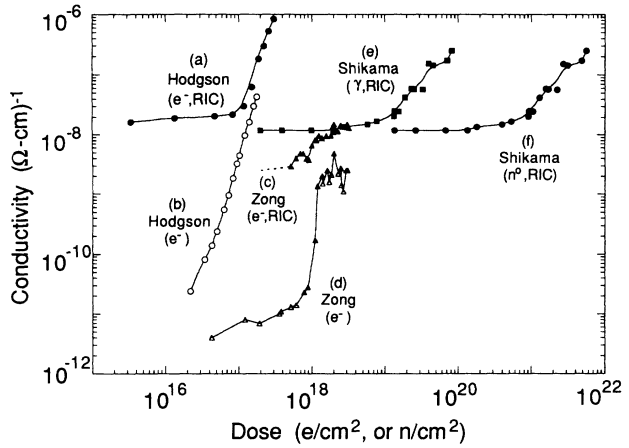

FIG. 9. Electrical conductivity vs electron or neutron dose in Al_2O_3 (a) during electron irradiation, Hodgson, Ref. 1; (b) post-electron-irradiation, Hodgson, Ref. 3; (c) during electron irradiation, Zong *et al.*, present study; (d) post electron irradiation, Zong *et al.*, present study; (e) ionizing γ dose in reactor in equivalent e/cm^2, Shikama *et al.*, Ref. 2; and (f) neutron dose with $E > 0.1$ MeV, Shikama *et al.*, Ref. 2. The electron dose rate for (c) is a factor of 20 as intense as that for (a). The equivalent e/cm^2 for ionizing γ dose rate in (e) is about the same as the electron dose rate in (c).

is based on the last conductivity measurement prior to the increase in conductivity signifying the onset of RIED. Even though curves (a) and (d) include RIC, and curve (b) does not, the magnitudes are correctly represented. The necessary condition is that the RIC contribution was constant. Comparing curves (a), (b), and (d) in Fig. 10, it is apparent that it requires 10^2–10^3 as many neutrons to cause RIED as one electron. This is an indication that RIED is dominated by the roles played by electrons and holes, rather than by knock-on displacements of indigenous ions.[14,15] If the RIED were caused by an elastic collision process, neutrons would have been much more efficient than electrons. Therefore we conclude that *in a fusion environment, it is the γ rays with the ensuing Compton electrons that cause the RIED.*

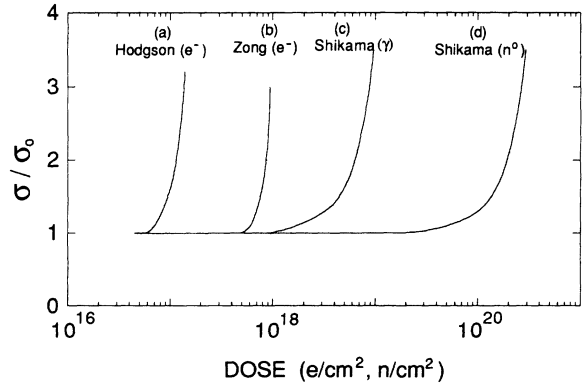

FIG. 10. Normalized conductivity, σ/σ_0, against e/cm^2 or n/cm^2 (a) electron irradiation, Ref. 1; (b) electron irradiation, present study; (c) equivalence of ionizing radiation in reactor, in e/cm^2, Ref. 2; and (d) neutron irradiation with neutron $E > 0.1$ MeV, in n/cm^2, Ref. 2.

B. Elastic collisions by 1.8-MeV electrons

Electrons with an energy of 1.8 MeV dissipate most of their energy in a crystal almost exclusively by ionization. Elastic collisions do occur but they constitute only a very small fraction of the energy loss. The critical dose for RIED to take place was reported to be $\sim 1 \times 10^{17}$ e/cm^2 in the earlier study, and a factor of 10 higher in the present work. These are small doses in terms of the ability of 1.8-MeV electrons to create sufficient displacements by elastic collisions to cause RIED. There are four factors that need to be considered: (1) elastic collisions by 1.8-MeV electrons in the oxides create negligible amounts of defects with order higher than monovacancy (see Refs. 14 and 15); that is, most of the defects produced are monovacancies. (2) A large fraction of the point defects created by elastic collisions from 1.8-MeV electrons do not survive thermal annihilation (due to interstitial-vacancy recombination) at 300 K or higher, especially in sapphire, as we shall see in the next section. (3) The range of 1.8-MeV electrons in sapphire is ~ 2.3 mm, indicating significant attenuation such that most of the damage is created in their initial paths. (4) The growth rate of the defect concentration with dose becomes strongly sublinear. Taking these four factors into consideration, we estimate that no more than 10^{15} vacancies/cm^3 can survive. This range of values is consistent with our post-mortem nondetection of anion vacancies, either by optical absorption or by magnetic resonance techniques—the latter being much more sensitive. It is highly unlikely that such small concentrations of vacancies can be responsible for RIED. Therefore we conclude that elastic collisions are not the primary mechanism.

C. Radiation damage in sapphire

In this section our discussions shall be based on the *assumption* that RIED is a radiation damage problem. Whether it is indeed a radiation damage problem or not is questionable and remains to be seen.

Each class of solid-state material is identified with its characteristic radiation damage mechanism. There are basically two types of mechanisms: those involving the collision of the incoming particles with the nuclei of the indigenous host (knock-ons or elastic collisions), and those involving the interaction of the incoming particles with electrons of the host ions (commonly referred to ionization, photochemical, or radiolysis process).[16] Both processes can displace indigeneous ions. The radiation damage processes in metals and semiconductors are known to be primarily due to elastic collisions, except where hydrogen is involved.[17,18] In insulators, both mechanisms can prevail, depending in general upon the type of crystals: halides or oxides. Halide crystals are generally characterized by ionization-induced displacements of halide ions.[19–22] Radiation damage in oxides such as MgO and Al_2O_3 are identified with elastic collisions,[23–27] except in the ionization-induced-displacements of substitutional protons and deuterons.[28–30] In oxide crystals, the resulting defects by elastic collisions are primarily associated with oxygen ions. Certainly cations are also displaced, but the resulting interstitials quickly recombine with vacancies.[14] Oxygen

ions are displaced, but generally only a small fraction survives subsequent interstitial-vacancy recombinations.

Even though the surviving point defects produced in Al_2O_3 are due to elastic collisions, the experimental results on RIED, in conjunction with the temperature dependence of radiation damage of insulating crystals in general, would lead one to believe that the mechanism leading to RIED is not associated with elastic collisions: The concentration of radiation-induced point defects depends on two factors, production efficiency and thermal stability. We shall discuss the production and thermal annihilation for defects produced by (a) elastic collisions, and (b) an ionization process.

(a) *Elastic collision:* For defects produced by elastic collisions, such as those in the oxides, the production rate is essentially independent of the temperature; that is, the production process is not thermally activated. The surviving defects, however, depend on the thermal stability of these defects, decreasing with increasing temperature. In the case of sapphire, thermal annealing also creates aggregate point defects at the expense of monovacancies, but nevertheless there is a net loss of defects. *Therefore, for defects produced by elastic collisions, increasing the irradiating temperature cannot result in a higher concentration of defects.*

(b) *Ionization:* For defects produced by an ionization mechanism, such as in the alkali halides, the production efficiency increases with temperature;[19] that is, the process is thermally activated. The surviving defects produced by an ionization mechanism also depend on the thermal stability, and decrease with increasing temperature. Similarly, aggregate defects can be created thermally, but again there is a net loss of point defects. *Therefore, for defects produced by an ionization mechanism, increasing the irradiating temperature can result in an increase of defect concentration.* One concludes that any observed increase in the concentration of defects with irradiating temperature is indicative of an ionization process.

Evidence is now provided in support of the argument that for defects produced by elastic collisions, a higher irradiation temperature cannot result in a higher concentration of defects. Experimental results from temperature dependence of neutron and electron irradiations are given as follows.

Neutron irradiation without an electric field: Results from experiments on neutron irradiations of Al_2O_3 and MgO crystals performed at two different temperatures indeed demonstrate that for defects produced by elastic collisions, irradiation at a higher temperature results in a lower surviving defect concentration. Optical-absorption measurements were performed after neutron irradiation on Al_2O_3 and MgO samples to monitor the surviving anion vacancies. The results are shown in Figs. 11, 12, and 13. In all three cases, neutron irradiations at higher temperatures, in spite of a higher dose, resulted in lower concentrations of anion vacancies. The mechanism associated with the production of these defects has been unambiguously identified with that of elastic collisions.[31]

Electron irradiation without an electric field: The threshold energy for elastic-collision displacements due to electron irradiation in sapphire is reported to be ~ 0.3 MeV,[32,33] corresponding to ~ 55 eV for the displacement of oxygen ions. Based on this value, the theoretical cross section for the displacement of oxygen for 1.8-MeV electrons is 8 b.[34] Knowing the theoretical cross section (σ), the fraction of the sublattice ions ($\Delta n/n$) can be calculated for a given dose ($\Delta\phi$), using the equation $\Delta n/n = \sigma\Delta\phi$. Using the critical dose of 1.3×10^{17} e/cm^2 (using the value of Ref. 1), a maximum displacement of 1 ppm of O^{2-} ions would have occurred when RIED began to take place. (Using our critical dose of 1.3×10^{17} e/cm^2 the value would be 10 ppm.) Theoretically obtained values of $\Delta n/n$, or σ, are always higher than their experimentally obtained counterparts, because the equation assumes zero interstitial-vacancy recombinations, and no energy attenuation as the electron penetrates the crystal. It is unrealistic to expect zero interstitial-vacancy recombination

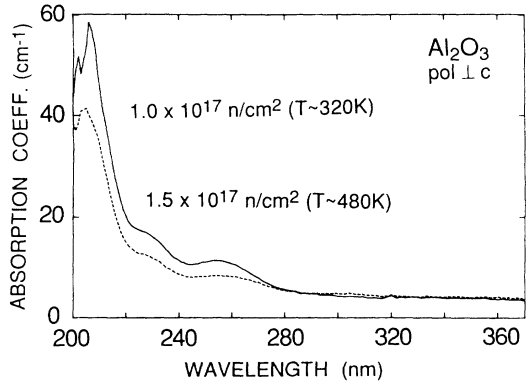

FIG. 11. Absorption coefficient vs wavelength for two neutron-irradiated Al_2O_3 crystals from UCC, one irradiated at 320 K (top curve), and the other at 480 K (bottom curve). The polarizer was oriented parallel to the c axis. The absorption at 205 nm is due to the two-electron anion vacancy (F center), and that at 258 nm due to the one-electron anion vacancy (F^+ center) (see Refs. 24–26).

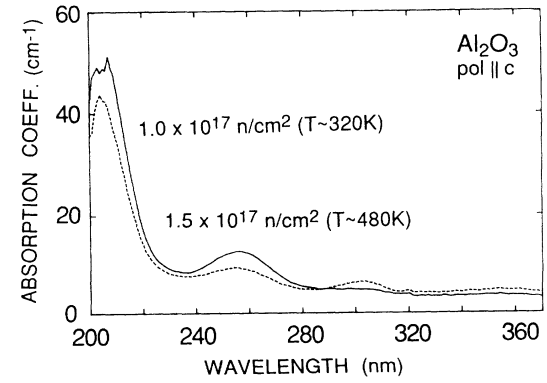

FIG. 12. Absorption coefficient vs wavelength for two neutron-irradiated Al_2O_3 crystals from UCC, one irradiated at 320 K (top curve), and the other at 480 K (bottom curve). The polarizer was oriented perpendicular to the c axis. The absorption at 205 nm is due to the F center, and that at 258 nm due to the F^+ center (see Refs. 24–26).

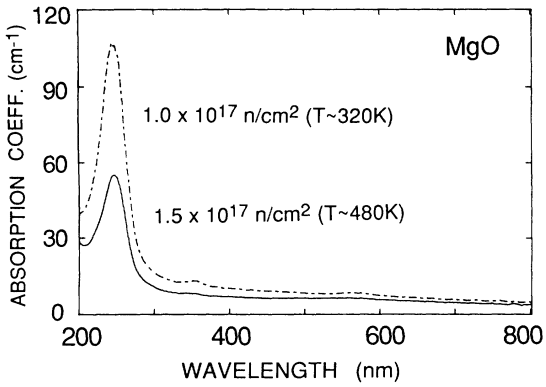

FIG. 13. Absorption coefficient vs wavelength for two neutron-irradiated MgO crystals grown at the ORNL, one irradiated at 320 K (top), and the other at 480 K (bottom). The absorption at 250 nm is due to both the F and F^+ centers (see Refs. 14 and 23). An absorption coefficient of 20 cm^{-1} corresponds to $\sim 1.0\times 10^{17}$ anion vacancies per cm^3 (see Refs. 14 and 15).

in radiation damage in solids.

An experiment was performed to estimate a realistic cross section, or the survival rate of anion vacancies in α-Al_2O_3 at room temperature for 1.8-MeV electron irradiation. Irradiation at room temperature was performed on a crystal from Union Carbide Corporation. The sample was placed in an irradiating chamber cooled with running water such that the temperature of the sample was maintained at 293 K. The total dose was $\sim 1\times 10^{19}$ e/cm^2, which is a factor of 3 greater than that used for the present RIED experiment and more than 30 times greater than that used in Ref. 1. The well-known F band (anion vacancy with 2 electrons) at ~ 205 nm was not observed. This means that no more than 0.05 ppm of oxygen vacancies were produced for this enormous dose. This value translates into an experimental cross section of 5×10^{-3} b, as compared to a theoretical value of 8b; that is, less than 1% of the oxygen vacancies survives thermal annihilation. To ascertain that it was not the irradiation facility that was responsible for the lack of defects observed, an MgO crystal was irradiated in the same facility; a large concentration of oxygen vacancies was observed.

Thus irradiation with energetic electrons produces low concentrations of oxygen vacancies in α-Al_2O_3 at room temperature by elastic collisions. We know that the concentration of defects produced by elastic collisions cannot increase at higher irradiating temperatures. Therefore if the problem is indeed due to radiation damage by elastic collision, in order to incur substantial damage at 773 K in the crystal of Ref. 1, or in the present study, it is necessary to impose another mechanism which is much more efficient—perhaps radiation damage by ionization.

D. RIED by γ rays in reactor

Reactor irradiations were performed by Shikama *et al.*[2] The data from his second experiment will be used for comparison, since those experimental conditions more closely resemble the two electron-irradiated Rad-E-T studies (see Table I). The background γ dose rate at the Japan Materials Test Reactor of Oarai Research Establishment of the Japan Atomic Energy Research Institute was reported to be $\sim 5.3\times 10^3$ Gy/s at full power. This γ dose can be converted into the equivalent 1.0-MeV electron dose. The conversion factor is 2.4×10^{-10} $Gy\,e^{-1}\,cm^2$ for the broad vicinity of 1-MeV γ rays.[13] Shikama's results are shown in Fig. 9(e) and Fig. 10(c). The RIED in the reactor began to occur at 2 days full power, which translates into 4×10^{18} e/cm^2. The ionizing component of the reactor epithermal neutrons (4.7×10^2 Gy/s) is small in comparison with that of the reactor γ radiation.[13] The two sets of electron Rad-E-T curves are shown as (a) and (b) in Fig. 10 for comparison. Two distinctions become apparent. First, the ionization from the γ rays from the reactor, curve (c), is not as efficient as that from electrons, but is within a factor of 10 of the present study. Second, the growth rate of the conductivity in curve (c) is not as rapid. There are possible explanations: In the first instance, the reactor study was based on polycrystalline material, whereas the present work was based on a single crystal. There is some evidence that polycrystalline materials may be more resilient to RIED than single crystals.[35] If this factor is considered, curve (c) could be surprisingly consistent with the present result, curve (b). In the second case, the reactor data encompass RIC, since these conductivity measurements were all performed in the reactor during full power operation. This additional component will tend to render an otherwise RIC-less slope less steep. The dose rate for our experiment (2.5×10^{13} $e\,cm^{-2}\,s^{-1}$) is very similar to the ionizing dose rate from γ rays (equivalent to 2.2×10^{13} $e\,cm^{-2}\,s^{-1}$). In fact, the slopes of the two curves during irradiation, labeled (c) Zong (e^-, RIC) and (e) Shikama (γ, RIC) in Fig. 9, are similar. Therefore we can tentatively conclude that curves (b) and (c) in Fig. 10 are consistent with one another, given that one is based on a single crystal and the other on polycrystalline material.

E. Energy dependence measurement

The strongest argument for the involvement of elastic collisions in the RIED of sapphire during Rad-E-T was the reported strong energy dependence of the electron irradiations on the electrical degradation.[1] In this study, 1.8-MeV electrons resulted in conductivity increase whereas 0.3-MeV electrons did not. The lower energy electrons correspond to the threshold energy below which no displacement of oxygen ions occurs by elastic collision.[32,33] The author therefore concluded that elastic collisions are necessary in the electrical breakdown.

This conclusion is not justified. The range of 0.3-MeV electrons is much smaller than the thickness of the samples, which was 1 mm. Whereas the 1.8-MeV electrons fully penetrated the sample, the 0.3-MeV electrons did not. Figure 14 shows the range in g/cm^2 (left ordinate) and in mm for sapphire (right ordinate) vs the energy of the irradiating electrons. The range of 0.3-MeV electrons in sapphire is 0.21 mm, which is only one-fifth of the

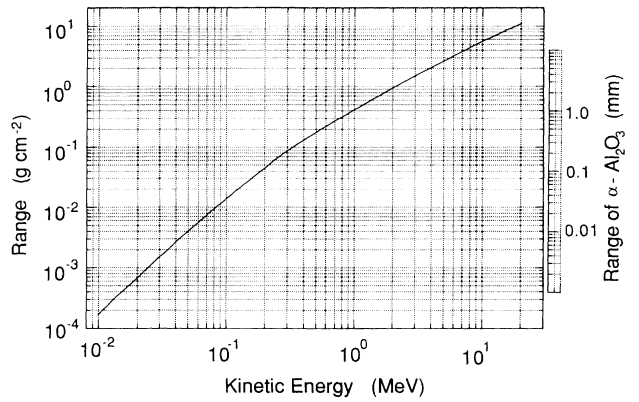

FIG. 14. Range vs energy of irradiating electrons [After Katz and Penfold, Rev. Mod. Phys. **24**, 28 (1952)]. Range of α-Al_2O_3 (in mm) is scaled on the right.

sample thickness. The conductivity of the sample during Rad-E-T was governed predominantly by the portion of the sample which was not irradiated. Regardless of how conducting the irradiated portion became, no substantial increase in conductivity through the bulk of the sample could occur. Therefore, no meaningful conclusion could be deduced from this experiment.

V. CONCLUSIONS

The present study addresses two fundamental questions. First, what is the defect associated with RIED? Second, what is the mechanism leading to RIED?

On the first issue, we depend in large part on the postmortem characterization of the sample after subjected to Rad-E-T. Three types of defects are discussed: (a) radiation-induced point defects, (b) second phase, and (c) dislocations.

(a) *Radiation-induced point defects, or vacancies:* It is highly unlikely that even a large concentration of vacancies (for example, $\sim 10^{19}$ anion vacancies cm^{-3}) will give rise to large increase in electrical conductivity, because the ground-state wave functions of the electronic states for these vacancies are compact. Our results showed that RIED occurred in the absence of vacancies ($< 10^{16}$ cm^{-3}), as monitored by optical-absorption and magnetic resonance techniques. It is highly unlikely that the optical absorption reported in Ref. 3 as the F^+ center (oxygen vacancy with one electron) has been correctly identified; the basis for our argument will be presented in a later publication.

(b) *Second phase:* In general, it is unlikely that precipitates will lead to RIED. The population of precipitates in the refractory oxides, if they exist, are low—typically no more than $\sim 10^{13}$ cm^{-3}, as monitored by TEM.[7–11] Earlier studies in MgO at high temperatures ($\sim$1473 K), with a moderate electric field but in the absence of radiation, demonstrate that electrical breakdown can occur without precipitates being formed.[36–38] Likewise, in the present study RIED occurred in a sample with no precipitates. Therefore we conclude that a second phase is not a prerequisite for RIED.

(c) *Dislocation:* There appears to be a correlation between the RIED and the preponderance of dislocations produced during Rad-E-T. In the shielded region (unirradiated and without an applied electric field) the dislocation density averaged $\sim 10^4$ cm^{-2}. This level of dislocation density is consistent with that found in virgin high-quality sapphire crystals. On the other hand, in the degraded region, which had been subjected to Rad-E-T, the dislocation density was exceedingly high. The dislocations were concentrated in high-density regions, but were estimated to have an *overall* average density of $\sim 10^9$ cm^{-2}. The observation of dislocations during Rad-E-T clearly indicates that RIED is a bulk effect, notwithstanding recent concerns on surface contamination.[39,40] Therefore we conclude that *the primary defects associated with RIED are dislocations generated during Rad-E-T.* However, we are not in a position to conclude whether dislocations are the cause or the consequence of RIED.

On the second issue, the implication of whether the mechanism leading to RIED is due to elastic collision or ionization are technically very important. In a first-generation fusion device, the particles of concern for ceramics are α, γ, and neutrons. The α particles are trapped at the first wall and are not expected to come in contact with the various ceramic components. A mechanism based on elastic collisions would indicate that neutrons would be the primary concern in causing RIED during the operation of a fusion device. If indeed both ionization and elastic collisions are necessary for RIED, as suggested in a previous study, then in order to suppress this catastrophy it is desirable to delay the process with the lower cross section, i.e., elastic collision. In brief, if displacements from elastic collisions are a prerequisite for RIED, then suppressing the role of neutrons would be the aim for any effort to diminish RIED. However, the results of the present study lead to our second conclusion, i.e., *RIED is caused primarily by the charge, or ionizing properties, of electrons and holes generated during electron irradiations, and not by elastic collisions with the energetic bombarding electrons, resulting in displacements of indigenous ions.* Therefore in any fusion environment, it is the γ rays which are primarily responsible for RIED. The technology involved in the safeguard against RIED therefore assumes a different complexity.

VI. SUMMARY AND CLOSING REMARKS

The goal of the present study is to obtain a better fundamental understanding of the mechanisms of RIED and the defects involved, particularly because of its important technological implications. The experimental conditions in our work were similar to the previous investigations using electrons,[1,3] but not identical. Both studies subjected sapphire to Rad-E-T (concurrent applications of electron radiation, electric field, and elevated temperature), and the magnitudes of the parameters were similar. On the other hand, there were several notable differences. First, the present experiments were carried out in an ambient atmosphere (air), whereas past experiments were performed in vacuum.[1] Second, our dose rate was about a factor of 20 higher. Third, the present irradiations

were carried out to a dose which was a factor of 10 higher. Fourth, there could have been a crystal orientation difference. Fifth, the sources of the sapphire crystals were different.

The basic observation of the earlier electron experiments has been confirmed, namely, that at some critical electron dose during Rad-E-T the electrical conductivity increases rapidly. However, there were some differences. First, the critical doses differed by a factor of 10. Second, in the earlier work it was reported that the crystal became dark, and that the coloration was related to the presence of precipitates. The crystal in the present study was colorless, suggesting an absence of Mie scattering and devoid of precipitates. TEM observations confirmed the absence precipitates. The different results are probably due to the presence or absence of oxygen surrounding the samples during Rad-E-T. The oxygen partial pressure is important in determining the defect structure and stoichiometry of metal oxides.[41] We propose that during Rad-E-T at 773 K the vapor pressure of oxygen is higher than that of aluminum, resulting in a net reduction process. The lack of precipitates in the present study indicates that RIED can occur without the presence of a second phase. Third, in the present work, irradiations were carried out beyond the dose at which the conductivity increased rapidly in the earlier work. In the previous work, the conductivity beyond that point was not reported, and the author assumed that the conductivity would increase until the sample suffers an electrical breakdown. The electrical conductivity in the present study, in fact, saturated at a value about 10^3 higher than in the virgin state. There was no indication that the conductivity would increase further at still higher doses, at least up to 1.4×10^{19} e/cm^2.

There are two main conclusions in the present study. First, the primary defects attending RIED are dislocations. We deduce that it is unlikely that radiation-induced vacancies, or a second phase, play an important role in RIED. Second, the mechanism leading to RIED is due to the charge of the electrons and holes created during irradiation, rather than due to displacements of indigenous ions by elastic collisions with the energetic bombarding electrons.

Since a guard ring was not used, and the conductivity was measured in air, some stray leakage currents may have been included in the post-irradiation conductivity value. This is evidenced by the relatively large values found for preirradiation conductivity in the present study (as well as in those experiments performed in vacuum, as reported in Refs. 1–4 and 12), when compared with recent results on sapphire by Will and Janora,[42] where a guard-ring technique was used in a vacuum maintained at 10^{-7} torr. On the other hand, the present experimental setup eliminates other related problems. First, the periphery of the sample was not subjected to Rad-E-T and therefore would not experience RIED. Secondly, the experiment was performed in air, so that no contamination from chemical decomposition of vacuum oil by electron irradiation would be deposited at the sample surface. Furthermore, the conditions employed herein realistically simulate some environments in which insulators are expected to function in future advanced energy devices. Therefore the present results are of interest to the fusion community dealing with these materials problems.

It is interesting to note that the factor of 10 difference in the critical dose for RIED in the two electron-irradiation experiments suggests that there is at least one variable, as yet unknown, which may help to extend the useful life of ceramics under Rad-E-T.

Finally, the present study demonstrates unambiguously that there can exist extensive damage to the bulk crystal during Rad-E-T. Nevertheless, recent investigators conclude that in their experiments the increase in conductivity was a result of radiation-induced surface contamination.[39,40] Regardless of the final outcome, the implications of their studies could well add another important dimension to electrical degradation in ceramics during irradiation.

ACKNOWLEDGMENTS

Research at the Oak Ridge National Laboratory was sponsored by the Division of Materials Sciences, U.S. Department of Energy under Contract No. DE-AC05-84OR21400 with Martin Marietta Energy Systems, Inc. Research at the Universidad Carlos III was supported by the Comision Interministerial de Ciencia y Tecnologia (CICYT) of Spain and by the Comunidad Autonoma de Madrid (CAM). Research at the Idaho National Engineering Laboratory was performed under Contract No. DE-AC07-76ID01570 with the Idaho Operations Office. The authors are indebted to M. M. Abraham for the electron-paramagnetic-resonance measurements. The authors gratefully acknowledge Frank Clinard for his critical reading of the manuscript and for his constructive comments.

---

*Also at the U.S. Department of Energy, ER-131, Division of Materials Sciences, Office of Basic Energy Sciences, Washington, D.C. 20585.

[1]E. R. Hodgson, J. Nucl. Mater. **179-181**, 383 (1991).

[2]T. Shikama, M. Narui, Y. Endo, T. Sagawa, and H. Kayano, J. Nucl. Mater. **191-194**, 575 (1992).

[3]E. R. Hodgson, *Proceedings of the XII International Conference on Defects in Insulating Materials*, edited by O. Kanert and J. M. Spaeth (World Scientific, Singapore, 1993), p. 332.

[4]G. P. Pells, J. Nucl. Mater. **179-181**, 383 (1991).

[5]R. W. Klaffky, B. H. Rose, A. N. Goland, and G. J. Dienes, Phys. Rev. B **21**, 3610 (1980).

[6]Y. Chen and F. W. Wiffen, DOE Task Force Meeting on Electrical Breakdown of Insulating Ceramics in a High-Radiation Field, ORNL Report No. CONF-9105176 (unpublished). During this meeting, it was recommended that this effect be generalized and termed radiation enhanced electrical degradation (REED), in order to distinguish it from RIC. It has

since been accepted by the fusion materials community that the phenomenon be referred to as radiation induced electrical degradation (RIED). The RIED acronym is used in this paper.

[7]C. Ballesteros, R. Gonzalez, S. J. Pennycook, and Y. Chen, Phys. Rev. B **38**, 4231 (1988).

[8]C. Ballesteros, R. Gonzalez, and Y. Chen, Phys. Rev. B **37**, 8008 (1988).

[9]C. Ballesteros, L. S. Cain, S. J. Pennycook, R. Gonzalez, and Y. Chen, Philos. Mag. **59**, 907 (1989).

[10]C. Ballesteros, R. Gonzalez, Y. Chen, and M. R. Kokta (unpublished).

[11]C. Ballesteros, R. Gonzalez, Y. Chen, and M. R. Kokta, Phys. Rev. B **47**, 2460 (1993).

[12]T. Shikama, M. Narui, A. Ochiai, H. Kayano, and Y. Endo, Sci. Rep. RITU, A **35**, 26 (1992).

[13]G. C. Messenger and M. S. Ash, *The Effects of Radiation on Electronic Systems* (Van Nostrand Reinhold, New York, 1986).

[14]W. A. Sibley and Y. Chen, Phys. Rev. **160**, 712 (1967).

[15]Y. Chen, D. L. Trueblood, O. E. Schow, and H. T. Tohver, J. Phys. C **3**, 2501 (1970).

[16]E. Sonder and W. A. Sibley, in *Defect in Crystalline Solids,* edited by J. H. Crawford, Jr. and L. M. Slifkin (Plenum, New York, 1972).

[17]W. L. Brown and W. M. Augustyniak, J. Appl. Phys. **30**, 1300 (1959).

[18]Y. Chen and J. W. MacKay, Phys. Rev. **167**, 745 (1968).

[19]R. T. Williams, K. S. Song, W. L. Faust, and C. H. Leung, Phys. Rev. B **33**, 7232 (1986).

[20]N. Itoh and K. Tanimura, J. Phys. Chem. Solids **51**, 717 (1990).

[21]J. M. Vail, J. Phys. Chem. Solids **51**, 589 (1990).

[22]R. T. Williams and K. S. Song, J. Phys. Chem. Solids **51**, 679 (1990).

[23]Y. Chen, M. M. Abraham, and D. F. Pedraza, Nucl. Instrum. Methods Phys. Res. Sec. B **59/60**, 1163 (1991).

[24]B. D. Evans and M. Stapelbroek, Phys. Rev. B **18**, 7079 (1978).

[25]B. D. Evans and M. Stapelbroek, J. Nucl. Mater. **85-86**, 497 (1979).

[26]B. D. Evans and M. Stapelbroek, Solid State Commun. **33**, 765 (1980).

[27]G. J. Pogatshnik, Y. Chen, and B. D. Evans, J. Lumin. **40/41**, 315 (1988).

[28]Y. Chen, M. M. Abraham, and H. T. Tohver, Phys. Rev. Lett. **37**, 1757 (1976).

[29]Y. Chen, R. Gonzalez, and K. L. Tsang, Phys. Rev. Lett. **53**, 1077 (1984).

[30]R. Gonzalez, E. R. Hodgson, C. Ballesteros, and Y. Chen, Phys. Rev. Lett. **67**, 2057 (1991).

[31]B. D. Evans, H. D. Hendricks, F. D. Bazzarre, and J. M. Bunch, *Ion Implantation in Semiconductor, 1976,* edited by Fred Chernow, James A. Borders, and David K. Brice (Plenum, New York, 1977), p. 265; J. H. Crawford, Jr., Semicond. Insulat. **5**, 599 (1983).

[32]G. W. Arnold and W. D. Compton, Phys. Rev. Lett. **4**, 66 (1960).

[33]K. J. Caulfield, R. Cooper, and J. F. Boas, J. Nucl. Mater. **184**, 150-151 (1991).

[34]O. S. Oen, Report No. ORNL-4897, Oak Ridge National Laboratory, Oak Ridge, Tenn., 1973 (unpublished).

[35]E. R. Hodgson, Radiat. Eff. Defect Solids, **119-121**, 827 (1991).

[36]K. L. Tsang, Y. Chen, and J. J. O'Dwyer, Phys. Rev. B **26**, 6909 (1982).

[37]K. L. Tsang and Y. Chen, J. Appl. Phys. **54**, 4531 (1983).

[38]K. L. Tsang, Y. Chen, and H. T. Tohver, Phys. Rev. B **30**, 6093 (1984).

[39]W. Kesternich, F. Scheuermann, and S. J. Zinkle, J. Nucl. Mater. **206**, 68 (1993).

[40]P. Jung, Z. Zhu, and H. Klein, J. Nucl. Mater. **206**, 72 (1993).

[41]P. Kofstad, *Non-stoichiometry, Diffusion and Electrical Conductivity in Binary Mixed Oxides* (Krieger, Malabar, FL, 1985).

[42]F. G. Will and K. J. Janora, J. Am. Cer. Soc. **75**, 2795 (1992).

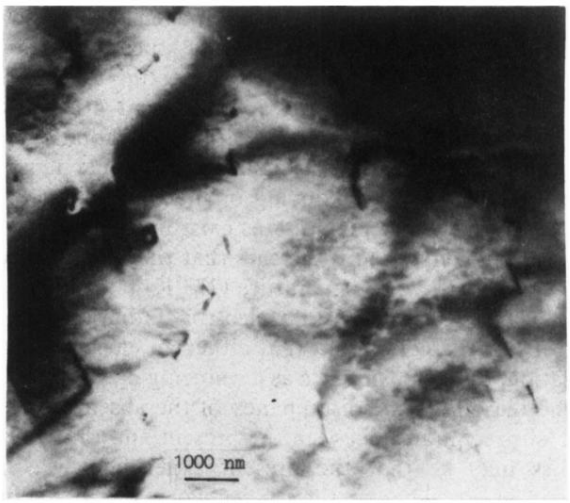

FIG. 7. Transmission electron micrograph showing high density of dislocations in an area previously subjected to Rad-E-T.

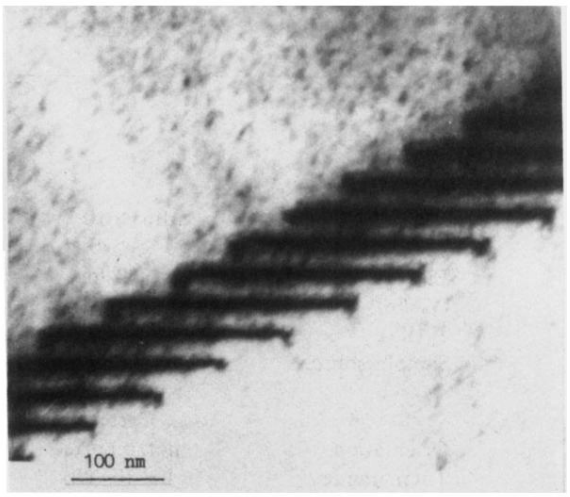

FIG. 8. Transmission electron micrograph of a low-angle boundary of dislocations in an area previously subjected to Rad-E-T.